Application of hyperbolic shear deformation theory to free vibration analysis of functionally graded porous plate with piezoelectric face-sheets

M. Arefi* and M. Meskini

Department of Solid Mechanic, Faculty of Mechanical Engineering, University of Kashan, Kashan 87317-51167, Iran

Abstract. In this paper, hyperbolic shear deformation theory is used for free vibration analysis of piezoelectric rectangular plate made of porous core. Various types of porosity distributions for the porous material is used. To obtain governing equations of motion, Hamilton's principle is used. The Navier's method is used to obtain numerical results of the problem in terms of significant parameters. One can conclude that free vibration responses are changed significantly with change of important parameters such as various porosities and dimensionless geometric parameters such as thickness to side length ratio and ratio of side lengths.

Keywords: free vibration; porous material; hyperbolic shear deformation theory; Hamilton's principle; porosity distribution

1. Introduction

The porous materials are combined of two elements as solid (body) and liquid or gas in which wood, stone, sponge and bone are example of these materials in the nature. Studies on the vibration response of porous FG structures, especially for beams and plates, are still limited in number. In recent decades, the use of piezoelectric materials combined with composites and functionally graded materials have been increased. One of the applications of these materials is vibration control and smart structures and systems (Chen *et al.* 2002). Static behavior of a FGM shell with a piezoelectric layer was investigated using higher-order shear deformation theories by Wu *et al.* (2002). Fakhari *et al.* (2011) investigated nonlinear vibration of FG plate with two piezoelectric layers under mechanical, electric and thermal loads using non-linear strain-displacement relations of von Karman and finite element method. Arefi and Zenkour (2017) studied the nonlocal thermo-magneto-electro-mechanical bending behaviors of nano sheet with two piezo-magnetic layers by using sinusoidal shear deformation plate theory.

Porous materials, such as metal foams, are an important category of lightweight materials with application to aerospace engineering. Usually, the variation of porosity through the thickness of porous plates causes a smooth change in mechanical properties. Abbas *et al.* (2015) studied two-dimensional problem of a porous material within the context of the fractional order generalized thermo-elasticity theory with one relaxation time. Ait Atmane *et al.* (2017) studied the use of an efficient beam theory for bending, free vibration and buckling analysis of functionally graded material (FGM) beams resting on two-parameter elastic foundation. Barati and Zenkour (2017)

investigated analysis of post-buckling behavior of porous metal foam nanobeams based on a nonlocal nonlinear refined shear deformation beam model with geometric nonlinearity and imperfection that in the metal foam nanobeam, porosities were simulated by uniform, symmetric and asymmetric models. Some important works on the application of higher-order shear deformation theory were published by various researchers (Reddy 2004, Benahmed *et al.* 2017, Elmeiche *et al.* 2011, Hebali *et al.* 2014). Some important relations of porous materials can be observed in literature (Galeban *et al.* 2016, Mirjavadi *et al.* 2017, Ebrahimi and Habibi, 2016).

According to strain gradient theory, the strain energy is a function of strain, strain gradients and material length scale parameters. Nonlocal strain gradient calibration of nanostructures via experiments and molecular dynamic simulation shows that their mechanical characteristics can be described using two scale parameters (Li *et al.* 2016, Mehralian *et al.* 2017, Lim *et al.* 2015). In fact, these two scale parameters consider the stiffness-softening and stiffness-hardening effects due to nonlocal stress field and strain gradients on mechanical behavior of nanostructures. Based on the nonlocal strain gradient theory, Li *et al.* (2015) studied the size-scaled effect on the wave propagation in functionally graded beams via the nonlocal strain gradient theory. Khorshidi *et al.* (2015) studied free vibration analysis of functionally graded rectangular nanoplates based on nonlocal exponential shear deformation theory. They indicated that some significant parameters such as nonlocal parameter, the ratio of the thickness to the length, the power law indexes and the aspect ratio have significant influence on the frequency values of a FG nano-plate. It's shown that the frequency ratio decreases with increasing the mode number and the value of the nonlocal parameter, and also increasing the power law index causes the non-dimensional frequencies to decrease. Mechab *et al.* (2016) presented free

---

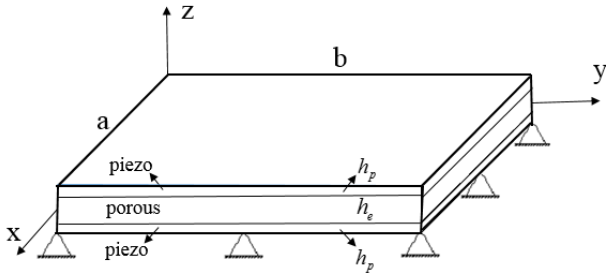*Corresponding author, Ph.D.
E-mail: arefi@kashanu.ac.ir

Fig. 1 The schematic figure of a sandwich porous plate

vibration analysis of FGM nanoplate with porosity resting on Winkler Pasternak elastic foundations based on two‑variable refined plate theories. They mentioned that the frequencies of the plates increase dramatically within the range of spring constant factors around 100 to 10. Additionally, the porosity within functionally graded plates is one of the important aspects that lead to considerable changes in frequencies. It has been indicated that the frequencies decrease as the porosity volume fraction increases for every value of the volume fraction index.

The literature review was completed above. This review indicates that free vibration analysis of sandwich plate including a porous core and two integrated piezoelectric layers has not been studied. In this paper, higher-order hyperbolic shear and normal deformation theory is used to derive governing equations of motion of a sandwich porous plate integrated with piezoelectric layers. Higher order shear deformation theory has sufficient capability with respect to lower order one for prediction the elastic deformations of sandwich structures. The higher order shear and normal deformation theory is used for more accurate variation of shear strains along the thickness direction. In addition to above advantage, this theory does not need to shear stress correction factor rather than first order shear deformation theory. The present paper and corresponding formulations are used for simulation of a sandwich thick porous plates including a FG porous core and two piezoelectric layers as sensor and actuator. The results of this paper can be used for measurement and control of vibration responses of porous structures. The porous materials are used in various structures due to high stiffness and low density that leads to highernatural frequencies. A parametric study is performed to obtain numerical results in terms of significant parameters such as porosity distribution and some dimensionless geometric parameters.

2. Fundamental equations

In the research, hyperbolic shear deformation theory is used. This theory is expressed (Benahmed *et al*. 2017)

$$
\begin{aligned}
u(x,y,t) &= u_0(x,y,t) - z\frac{\partial w_b}{\partial x} - f(z)\frac{\partial w_s}{\partial x} \\
v(x,y,t) &= v_0(x,y,t) - z\frac{\partial w_b}{\partial y} - f(z)\frac{\partial w_s}{\partial y} \\
w(x,y,t) &= w_b(x,y,t) + w_s(x,y,t) + g(z)\varphi(x,y,t)
\end{aligned} \tag{1}
$$

Where u, v, w are the displacement components along x, y and z direction (Figure 1), respectively and w_b, w_s are the bending and shear portions of the transvers displacement.

In addition, φ is displacement of the effect of normal stress and $f(z)$, $g(z)$ are shape functions that are expressed as: (Benahmed *et al*. 2017)

$$
f(z) = \frac{\left(\dfrac{h}{\pi}\right)\sinh\left(\dfrac{\pi}{h}z\right) - z}{\cosh\left(\dfrac{\pi}{2}\right) - 1}, g(z) = 1 - f'(z) \tag{2}
$$

Strain-displacement relations are expressed

$$
\begin{cases}
\varepsilon_x = \dfrac{\partial u}{\partial x} = \dfrac{\partial u_0}{\partial x} - z\dfrac{\partial^2 w_b}{\partial^2 x} - f(z)\dfrac{\partial^2 w_s}{\partial^2 x} \\[2mm]
\varepsilon_y = \dfrac{\partial v}{\partial y} = \dfrac{\partial v_0}{\partial y} - z\dfrac{\partial^2 w_b}{\partial^2 y} - f(z)\dfrac{\partial^2 w_s}{\partial^2 y} \\[2mm]
\gamma_{xy} = \dfrac{\partial u}{\partial y} + \dfrac{\partial v}{\partial x} = \dfrac{\partial u_0}{\partial y} + \dfrac{\partial v_0}{\partial x} - 2z\dfrac{\partial^2 w_b}{\partial x\partial y} - 2f(z)\dfrac{\partial^2 w_s}{\partial x\partial y} \\[2mm]
\gamma_{xz} = \dfrac{\partial u}{\partial z} + \dfrac{\partial w}{\partial x} = g(z)\dfrac{\partial w_s}{\partial x} + g(z)\dfrac{\partial \varphi}{\partial x} \\[2mm]
\gamma_{yz} = \dfrac{\partial v}{\partial z} + \dfrac{\partial w}{\partial x} = g(z)\dfrac{\partial w_s}{\partial y} + g(z)\dfrac{\partial \varphi}{\partial y}
\end{cases} \tag{3}
$$

Electric-displacement relations for piezoelectric layers are defined (Arefi and Rahimi 2012, Arefi 2016, Arefi and Zenkour 2017a, b)

$$
\begin{bmatrix} D_x \\ D_y \\ D_z \end{bmatrix} = \begin{bmatrix} 0 & 0 & 0 & e_{15} & 0 \\ 0 & 0 & 0 & 0 & e_{26} \\ e_{13} & e_{32} & 0 & 0 & 0 \end{bmatrix} \begin{Bmatrix} \varepsilon_x \\ \varepsilon_y \\ \gamma_{xy} \\ \gamma_{xz} \\ \gamma_{yz} \end{Bmatrix}
$$
$$
+ \begin{bmatrix} \in_{11} & 0 & 0 \\ 0 & \in_{22} & 0 \\ 0 & 0 & \in_{33} \end{bmatrix} \begin{Bmatrix} E_x \\ E_y \\ E_z \end{Bmatrix} \tag{4}
$$

Where e_{ij} are the piezoelectric coefficients, E_i are the electric field components and $\in_{ij}$ are the dielectric coefficients. The electric field components are defined

$$
\begin{cases}
E_x = -\dfrac{\partial \hat{\psi}}{\partial x} \\[2mm]
E_y = -\dfrac{\partial \hat{\psi}}{\partial y} \\[2mm]
E_z = -\dfrac{\partial \hat{\psi}}{\partial z}
\end{cases} \tag{5}
$$

In which $\hat{\Psi}$ is electric potential that is defined as follows:

$$
\begin{cases}
\hat{\psi} = -\dfrac{2\hat{z}}{h_p}\psi_0 - \psi(x,y,t)\cos\left(\dfrac{\pi \hat{z}}{h_p}\right) \\[2mm]
\hat{z} = z - \dfrac{h_p}{2}, \hat{z} = z + \dfrac{h_p}{2}
\end{cases} \tag{6}
$$

In Eq. (6), Ψ_0 is initial electric potential at top of piezoelectric layers. Electric fields are derived by substitution of Eq. 6 into Eq. 5 as follows:

$$\begin{cases} E_x = -\dfrac{\partial \hat{\psi}}{\partial x} = \dfrac{\partial \psi}{\partial x} \cos\left(\dfrac{\pi \hat{z}}{h}\right) \\[3mm] E_y = -\dfrac{\partial \hat{\psi}}{\partial y} = \dfrac{\partial \psi}{\partial y} \cos\left(\dfrac{\pi \hat{z}}{h}\right) \\[3mm] E_z = -\dfrac{\partial \hat{\psi}}{\partial z} = -\dfrac{2}{h_p} \psi_0 - \psi \sin\left(\dfrac{\pi \hat{z}}{h}\right) \end{cases} \tag{7}$$

Different types of porosity distributions for the porous material is expressed (Rezaei and Saidi 2016, Barati and Zenkour 2017, Li *et al.* 2018, Chen *et al.* 2019)

1-Uniform porosity distribution

$$\begin{cases} E = E_1 - (1 - e_0 \chi) \\ G = G_1 - (1 - e_0 \chi) \\ \rho = \rho_1 - \sqrt{(1 - e_0 \chi)} \end{cases} \tag{8a}$$

2- Non-uniform distribution1

$$\begin{cases} E(z) = E_1 - \left(1 - e_0 \cos\left(\dfrac{\pi z}{h}\right)\right) \\[2mm] G(z) = G_1 - \left(1 - e_0 \cos\left(\dfrac{\pi z}{h}\right)\right) \\[2mm] \rho(z) = \rho_1 - \left(1 - e_m \cos\left(\dfrac{\pi z}{h}\right)\right) \end{cases} \tag{8b}$$

3- Non-uniform distribution 2

$$\begin{cases} E(z) = E_1 - \left(1 - e_0 \cos\left(\dfrac{\pi z}{2h} + \dfrac{\pi}{4}\right)\right) \\[2mm] G(z) = G_1 - \left(1 - e_0 \cos\left(\left(\dfrac{\pi z}{2h} + \dfrac{\pi}{4}\right)\right)\right) \\[2mm] \rho(z) = \rho_1 - \left(1 - e_m \cos\left(\left(\dfrac{\pi z}{2h} + \dfrac{\pi}{4}\right)\right)\right) \end{cases} \tag{8c}$$

where E, G, ρ are elasticity moduli, shear moduli and density; e_0, e_m are the coefficients of porosity and mass density and coefficient of uniform porosity distribution χ are defined as (Zhao *et al.* 2018)

$$\begin{cases} e_0 = 1 - \dfrac{E_2}{E_1} = 1 - \dfrac{G_2}{G_1} \\[2mm] e_m = 1 - \dfrac{\rho_2}{\rho_1} \\[2mm] \dfrac{E_2}{E_1} = \left(\dfrac{\rho_2}{\rho_1}\right)^2 \\[2mm] e_m = \sqrt{1 - e_0} \\[2mm] \chi = \dfrac{1}{e_0} - \dfrac{1}{e_0}\left(\dfrac{2}{\pi}\sqrt{1 - e_0} - \dfrac{2}{\pi} + 1\right)^2 \end{cases} \tag{9}$$

Stress-strain relations for core (porous material) are defined

$$\begin{bmatrix} \sigma_x \\ \sigma_y \\ \tau_{xy} \\ \tau_{xz} \\ \tau_{yz} \end{bmatrix} = \begin{bmatrix} c_{11} & c_{12} & 0 & 0 & 0 \\ c_{12} & c_{22} & 0 & 0 & 0 \\ 0 & 0 & c_{66} & 0 & 0 \\ 0 & 0 & 0 & c_{44} & 0 \\ 0 & 0 & 0 & 0 & c_{55} \end{bmatrix} \begin{Bmatrix} \varepsilon_x \\ \varepsilon_y \\ \gamma_{xy} \\ \gamma_{xz} \\ \gamma_{yz} \end{Bmatrix} \tag{10}$$

Stress-strain relation for piezoelectric layers are defined (Arefi and Zenkour 2017)

$$\begin{bmatrix} \sigma_x \\ \sigma_y \\ \tau_{xy} \\ \tau_{xz} \\ \tau_{yz} \end{bmatrix} = \begin{bmatrix} c_{11} & c_{12} & 0 & 0 & 0 \\ c_{12} & c_{22} & 0 & 0 & 0 \\ 0 & 0 & c_{66} & 0 & 0 \\ 0 & 0 & 0 & c_{44} & 0 \\ 0 & 0 & 0 & 0 & c_{55} \end{bmatrix} \begin{Bmatrix} \varepsilon_x \\ \varepsilon_y \\ \gamma_{xy} \\ \gamma_{xz} \\ \gamma_{yz} \end{Bmatrix}$$
$$- \begin{bmatrix} 0 & 0 & e_{13} \\ 0 & 0 & e_{23} \\ 0 & 0 & 0 \\ e_{51} & 0 & 0 \\ 0 & e_{62} & 0 \end{bmatrix} \begin{Bmatrix} E_x \\ E_y \\ E_z \end{Bmatrix} \tag{11}$$

Also, Hamilton's principle expresses that (Demirhan and Taskin 2018)

$$\int_{t_1}^{t_2} (\delta U - \delta T - \delta W) dt = 0 \tag{12}$$

Where U is the strain energy, T is the kinetic energy of the plate and W is the work of external force. Variation of strain energy is defined

$$\delta U = \int_v \left(\sigma_{ij} \delta\varepsilon_{ij} - D_i \delta E_i\right) dV$$
$$= \int_v \begin{pmatrix} \sigma_x \delta\varepsilon_x + \sigma_x \delta\varepsilon_x + \tau_{xy} \delta\gamma_{xy} + \tau_{xz} \delta\gamma_{xz} + \tau_{yz} \delta\gamma_{yz} \\ -D_x \delta E_x - D_y \delta E_y - D_z \delta E_z \end{pmatrix} dV \tag{13}$$

Variation of kinetic energy is defined as (Kim *et al.* 2019)

$$\delta T = \int_v \rho \vec{v} . \delta\vec{v}\, dV \tag{14}$$

The variation of U, T are presented in Appendix1 and 2. With substitution of variation of strain energy and kinetic energy to Hamilton's principle, equations of motion are obtained as

$$\delta u_0 : \frac{\partial N_x}{\partial x} + \frac{\partial N_{xy}}{\partial y} = I_1 \ddot{u}_0 - I_2 \ddot{w}_{b,x} - I_4 \ddot{w}_{s,x}$$

$$\delta v_0 : \frac{\partial N_{xy}}{\partial x} + \frac{\partial N_y}{\partial y} = I_1 \ddot{v}_0 - I_2 \ddot{w}_{b,y} - I_4 \ddot{w}_{s,y} \tag{15}$$

$$\delta w_b : \frac{\partial^2 M_x^b}{\partial x^2} + \frac{\partial^2 M_y^b}{\partial y^2} + 2\frac{\partial^2 M_{xy}^b}{\partial x \partial y} =$$

$$I_1 \ddot{w}_b + I_1 \ddot{w}_s + I_2 \ddot{u}_{0,x} + I_2 \ddot{v}_{0,y}$$

$$-I_3 \ddot{w}_{b,xx} - I_3 \ddot{w}_{b,yy} - I_5 \ddot{w}_{s,xx} - I_5 \ddot{w}_{s,yy} + I_7 \ddot{\varphi}$$

$$\delta w_s : \frac{\partial^2 M_x^b}{\partial x^2} + \frac{\partial^2 M_y^b}{\partial y^2} + 2\frac{\partial^2 M_{xy}^b}{\partial x \partial y} + \frac{\partial S_{xz}}{\partial x} + \frac{\partial S_{yz}}{\partial y} =$$

$$I_1 \ddot{w}_b + I_1 \ddot{w}_s + I_4 \ddot{u}_{0,x} + I_4 \ddot{v}_{0,y}$$

$$-I_5 \ddot{w}_{b,xx} - I_5 \ddot{w}_{b,yy} - I_6 \ddot{w}_{s,xx} - I_6 \ddot{w}_{s,yy} + I_7 \ddot{\varphi}$$

$$\delta\varphi : \frac{\partial S_{xz}}{\partial x} + \frac{\partial S_{yz}}{\partial y} = I_7 \ddot{w}_b + I_7 \ddot{w}_s + I_8 \ddot{\varphi}$$

$$\delta\psi : \frac{\partial P_x}{\partial x} + \frac{\partial P_y}{\partial y} - R_z = 0$$

In which the resultant components N_i, M_i^b, M_i^s, S_{ij}, P_i, R_i are given by

$$\begin{cases} \int \sigma_i dz = N_i, (i = x, y, xy) \\ \int \sigma_i z dz = M_i^b, (i = x, y, xy) \\ \int \sigma_i f(z) dz = M_i^s, (i = x, y, xy) \\ \int \tau_{ij} g(z) dz = S_{ij}, (ij = xz, yz) \\ \int D_i \cos\left(\frac{\pi z}{h}\right) dz = P_i, (i = x, y) \\ \int D_i \frac{\pi}{h_p} \sin\left(\frac{\pi z}{h}\right) dz = R_i, (i = z) \end{cases} \quad (16)$$

The integration constant expressed in Eq. (15) are defined as follows:

$$\{I_1, I_2, I_3, I_4, I_5, I_6, I_7, I_8\} =$$
$$\int \left(1, z, z^2, f(z), zf(z), f(z)^2, g(z), g(z)^2\right)\rho(z) dz$$

$$\{A_i, B_i, D_i, E_i, F_i, G_i, H_i\} =$$
$$\int \left(1, z, z^2, f(z), zf(z), f(z)^2, g(z)^2\right)c_i dz$$

$$L_{ij}^5 = \int (\cos(\frac{\hat{\pi z}}{h_p}))^2 e_{ij} dz, \ L_{ij}^3 = \int \cos(\frac{\hat{\pi z}}{h_p}).g(z) e_{ij} dz, \quad (17)$$

$$K_{ij}^5 = \int (\frac{\pi}{h_p} \sin(\frac{\hat{\pi z}}{h_p}))^2 e_{ij} dz, \ K_{ij}^1 = \int (\frac{\pi}{h_p} \sin(\frac{\hat{\pi z}}{h_p}))e_{ij} dz,$$

$$K_{ij}^2 = \int \frac{\pi}{h_p} \sin(\frac{\hat{\pi z}}{h_p}).z \, e_{ij} dz, \ K_{ij}^4 = \int \frac{\pi}{h_p} \sin(\frac{\hat{\pi z}}{h_p})f(z) e_{ij} dz$$

The governing equations of motion for piezoelectric-porous plate are obtained by introducing Eqs. (16), (12), (11) into Eq. (15) as follow:

$$\delta u : A_{11} \frac{\partial^2 u}{\partial x^2} + A_{66} \frac{\partial^2 u}{\partial y^2} + (A_{12} + A_{66}) \frac{\partial^2 v}{\partial x \partial y} - B_{11} \frac{\partial^3 w_b}{\partial x^3}$$

$$-(B_{12} + 2B_{66}) \frac{\partial^3 w_b}{\partial x \partial y^2} - (E_{12} + 2E_{66}) \frac{\partial^3 w_s}{\partial x \partial y^2} - E_{11} \frac{\partial^3 w_s}{\partial x^3} \quad (18a)$$

$$+K_{13}^1 \frac{\partial \psi}{\partial x} = I_1 \ddot{u} - I_2 \ddot{w}_{b,x} - I_4 \ddot{w}_{s,x}$$

$$\delta v : (A_{12} + A_{66}) \frac{\partial^2 u}{\partial x \partial y} + A_{66} \frac{\partial^2 v}{\partial x^2} + A_{22} \frac{\partial^2 v}{\partial y^2}$$

$$+(B_{12} + 2B_{66}) \frac{\partial^3 w_b}{\partial x^2 \partial y} - B_{22} \frac{\partial^2 w_b}{\partial y^3} + -(E_{12} + 2E_{66}) \frac{\partial^3 w_s}{\partial x^2 \partial y} \quad (18b)$$

$$-E_{22} \frac{\partial^3 w_s}{\partial y^3} + K_{23}^1 \frac{\partial \psi}{\partial y} = I_1 \ddot{v} - I_2 \ddot{w}_{b,y} - I_4 \ddot{w}_{s,y}$$

$$\delta w_b : B_{11} \frac{\partial^3 u}{\partial x^3} + (B_{12} + 2B_{66}) \frac{\partial^3 u}{\partial x \partial y^2} + (B_{12} + 2B_{66}) \frac{\partial^3 v}{\partial x^2 \partial y}$$

$$-B_{22} \frac{\partial^3 v}{\partial y^3} - D_{11} \frac{\partial^4 w_b}{\partial x^4} - D_{22} \frac{\partial^4 w_b}{\partial y^4} - (2D_{12} + 4D_{66}) \frac{\partial^4 w_b}{\partial x^2 \partial y^2}$$

$$-F_{11} \frac{\partial^4 w_s}{\partial x^4} - F_{22} \frac{\partial^4 w_s}{\partial y^4} - (2F_{12} + 4F_{66}) \frac{\partial^4 w_s}{\partial x^2 \partial y^2} + K_{13}^2 \frac{\partial^2 \psi}{\partial x^2} \quad (18c)$$

$$+K_{23}^2 \frac{\partial^2 \psi}{\partial y^2} = I_1 \ddot{w}_b + I_1 \ddot{w}_s + I_2 \ddot{u}_{0,x} + I_2 \ddot{v}_{0,y} - I_3 \ddot{w}_{b,xx}$$

$$-I_3 \ddot{w}_{b,yy} - I_5 \ddot{w}_{s,xx} - I_5 \ddot{w}_{s,yy} + I_7 \ddot{\varphi}$$

$$\delta w_s : E_{11} \frac{\partial^3 u}{\partial x^3} + (E_{12} + 2E_{66}) \frac{\partial^3 u}{\partial x \partial y^2} + (E_{12} + 2E_{66}) \frac{\partial^3 v}{\partial x^2 \partial y}$$

$$+E_{22} \frac{\partial^3 v}{\partial y^3} - F_{11} \frac{\partial^4 w_b}{\partial x^4} - F_{22} \frac{\partial^4 w_b}{\partial y^4} - (2F_{12} + 4F_{66}) \frac{\partial^4 w_b}{\partial x^2 \partial y^2}$$

$$-(2G_{12} + 4G_{66}) \frac{\partial^4 w_s}{\partial x^2 \partial y^2} - G_{22} \frac{\partial^4 w_s}{\partial y^4} + H_{44} \frac{\partial^2 w_s}{\partial x^2} + H_{55} \frac{\partial^2 w_s}{\partial y^2}$$

$$+H_{44} \frac{\partial^2 \varphi}{\partial x^2} + H_{55} \frac{\partial^2 \varphi}{\partial y^2} + K_{13}^4 \frac{\partial^2 \psi}{\partial x^2} + K_{23}^4 \frac{\partial^2 \psi}{\partial y^2} - L_{51}^3 \frac{\partial^2 \psi}{\partial x^2} \quad (18d)$$

$$+L_{62}^3 \frac{\partial^2 \psi}{\partial y^2} = I_1 \ddot{w}_b + I_1 \ddot{w}_s + I_4 \ddot{u}_{0,x} + I_4 \ddot{v}_{0,y} - I_5 \ddot{w}_{b,xx}$$

$$-I_5 \ddot{w}_{b,yy} - I_6 \ddot{w}_{s,xx} - I_6 \ddot{w}_{s,yy} + I_7 \ddot{\varphi}$$

$$\delta\varphi : H_{44} \frac{\partial^2 w_s}{\partial x^2} + H_{55} \frac{\partial^2 w_s}{\partial y^2} + H_{44} \frac{\partial^2 \varphi}{\partial x^2} + H_{55} \frac{\partial^2 \varphi}{\partial y^2}$$

$$-L_{51}^3 \frac{\partial^2 \psi}{\partial x^2} + L_{62}^3 \frac{\partial^2 \psi}{\partial y^2} = I_7 \ddot{w}_b - I_7 \ddot{w}_s + I_8 \ddot{\varphi} \quad (18e)$$

$$\delta\psi : K_{13}^1 \frac{\partial u}{\partial x} + K_{23}^1 \frac{\partial v}{\partial y} - K_{13}^2 \frac{\partial^2 w_b}{\partial x^2} - K_{23}^2 \frac{\partial^2 w_b}{\partial y^2}$$

$$+(L_{51}^3 - K_{13}^4) \frac{\partial^2 w_s}{\partial y^2} + L_{51}^3 \frac{\partial^2 \varphi}{\partial x^2} \quad (18f)$$

$$+L_{62}^3 \frac{\partial^2 \varphi}{\partial y^2} + L_{11}^5 \frac{\partial^2 \psi}{\partial x^2} + L_{22}^5 \frac{\partial^2 \psi}{\partial y^2} - K_{33}^5 \psi = 0$$

3. Solution Procedure

To study the influence of significant parameters such as porosity characteristics and dimensionless geometric parameters on the free vibration characteristics, the numerical results are presented based on analytical method. For this purpose, the Navier's solution is expressed as

$$v_0 = w_b = w_s = \frac{\partial w_s}{\partial y} = \varphi = N_x = M_x^b = M_x^s = 0 \ at \ x = 0, a$$

$$(19)$$

$$u_0 = w_b = w_s = \frac{\partial w_s}{\partial x} = \varphi = N_y = M_y^b = M_y^s = 0 \ at \ y = 0, b$$

Table 1 variation of non-dimensional natural frequencies of sandwich porous plate in terms of various thickness to side length ratio h/a

h/a		P (power-law exponent)				
		0	0.5	1	4	10
0.05	Present	0.016	0.0136	0.0122	0.0105	0.01002
	Ref (Benachour *et al*. 2011)	0.0148	0.0125	0.0113	0.0098	0.0094
0.1	Present	0.062	0.053	0.047	0.040	0.038
	Ref (Benachour *et al*. 2011)	0.0576	0.049	0.044	0.038	0.036
0.2	Present	0.228	0.196	0.176	0.147	0.138
	Ref (Benachour *et al*. 2011)	0.211	0.180	0.162	0.137	0.130

Table 2 Variation of natural frequencies in terms of side length ratio a/b for various porosities

ratio	0.1	0.25	0.5	1	2	3	4	5
Uniform	68465.405	29400.317	17448.533	14069.140	17650.306	23498.537	29879.552	36445.568
Nonuniform1	69026.851	29654.244	17604.994	14201.908	17822.666	23728.888	30171.601	36800.016
Nonuniform2	68590.000	29454.195	17481.252	14096.757	17686.253	23546.859	29941.216	36520.912

The Navier's solution procedure is expressed for simply-supported boundary condition as follows (Arefi and Zenkour 2017a, b, Arefi and Zenkour 2018, Arefi *et al* 2018, Arefi 2018a, b):

$$\begin{Bmatrix} u_0 \\ v_0 \\ w_b \\ w_s \\ \varphi \\ \psi \end{Bmatrix} = \begin{Bmatrix} Ue^{iwt}\cos\lambda x\sin\mu y \\ Ve^{iwt}\sin\lambda x\cos\mu y \\ W_b e^{iwt}\sin\lambda x\sin\mu y \\ W_s e^{iwt}\sin\lambda x\sin\mu y \\ \varphi e^{iwt}\sin\lambda x\sin\mu y \\ \psi e^{iwt}\sin\lambda x\sin\mu y \end{Bmatrix}, \lambda = \frac{n\pi}{a}, \mu = \frac{m\pi}{b} \quad (20)$$

Where U, V, W_b, W_s, φ, Ψ are unknown amplitudes and m, n denote the number of axial and transverse waves in the mode shapes and ω is the natural frequency of vibration.

By introducing equation (20) Into equation (18), two 6 ×6 displacement coefficient matrix can be expressed

$$[K]_{6\times 6} - \omega^2 [M]_{6\times 6} = 0 \quad (21)$$

The component of [K], [M] are presented in appendix 3.

4. Numerical results and discussions

In this section the obtained results of free vibration for a porous sandwich plate with simply support boundary conditions are presented. The core is considered porous material and three properties of the material are considered as $E = 200 \times 10^9 (N/m^2), v = 0.3, \rho = 7850(kg/m^3)$.

Furthermore, the properties of piezoelectric layers are considered as follows:

$$c_{11} = 226GPa, c_{22} = 226GPa, c_{12} = 125GPa,$$
$$c_{44} = 44.2GPa, c_{55} = 44.2GPa, c_{66} = 50.5GPa$$
$$e_{13} = -2.2(C/m^2), e_{23} = -2.2(C/m^2),$$
$$e_{26} = 5.8(C/m^2), e_{15} = -5.8(C/m^2)$$
$$\epsilon_{11} = 5.64 \times 10^{-9}(C/Vm), \epsilon_{22} = 5.64 \times 10^{-9}(C/Vm),$$
$$\epsilon_{33} = 6.35 \times 10^{-9}(C/Vm)$$

Before presentation of full numerical results, the governing equations and corresponding numerical results should be validated. A comparison with existing reference is presented for validation of numerical results (Benachour *et al*. 2011). Table 1 lists variation of non-dimensional natural frequencies of sandwich porous plate in terms of various thickness to side length ratio h/a based on the present and previous results (Benachour *et al*. 2011). This comparison indicates that the present numerical results are in good agreement with literature results.

Table 2 lists variation of natural frequencies in terms of side length ratio a/b for various porosities. It is noted that with change of side length ratio a/b, the area of plate is assumed constant ($a \times b = Const$). It is observed that the second distribution (Nonuniform1) yields highest natural frequency and lowest one is reached for first distribution (Uniform). In addition, the lowest natural frequency is obtained for a/b=1 and for the side length ratios greater than a/b=1, the natural frequencies are increased significantly.

Shown in Figure 2 is variation of first, second and third natural frequencies of sandwich porous plate in terms of various values of side length ratio a/b. The numerical results show that the lowest values of natural frequencies are obtained for a/b=1. To study the influence of thickness of core and piezoelectric layers on the vibration characteristics of sandwich porous plate, the ratio of core thickness to piezoelectric thickness h_e/h_p is selected. Table 3 lists variation of natural frequencies in terms of various values of h_e/h_p for different porosities. The results of Table 3 are obtained for the case that total thickness of plate is assumed constant ($h_e + 2h_p = Const$). The numerical results indicate that with increase of h_e/h_p, the natural frequencies are decreased significantly. One can conclude that with increase of h_e/h_p the stiffness of sandwich plate is decreased and consequently the natural frequencies are decreased.

Shown in Figure 3 is variation of first, second and third natural frequencies of sandwich porous plate in terms of h_e/h_p ratio. The numerical results indicate that with increase of h_e/h_p ratio, the natural frequencies for various modes are decrease smoothly. To investigate the influence of side length to thickness ratio a/h, Table 4 lists variation of fundamental natural frequencies of sandwich porous plate in terms of various a/h for different porosity distributions.
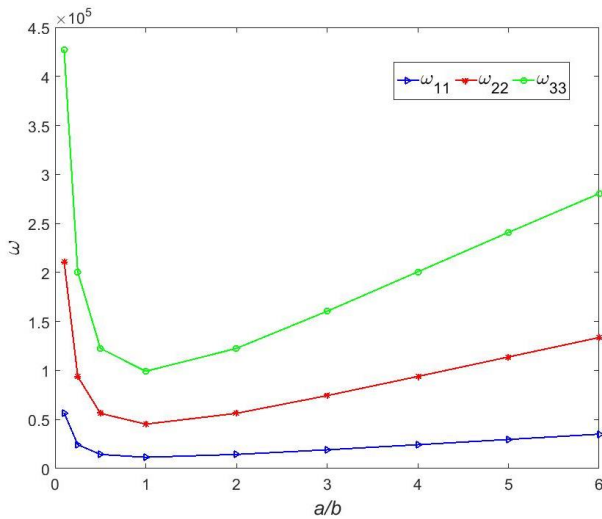
Fig. 2 Variation of first, second and third natural frequencies of sandwich porous plate in terms of variousvalues of side length ratio a/b
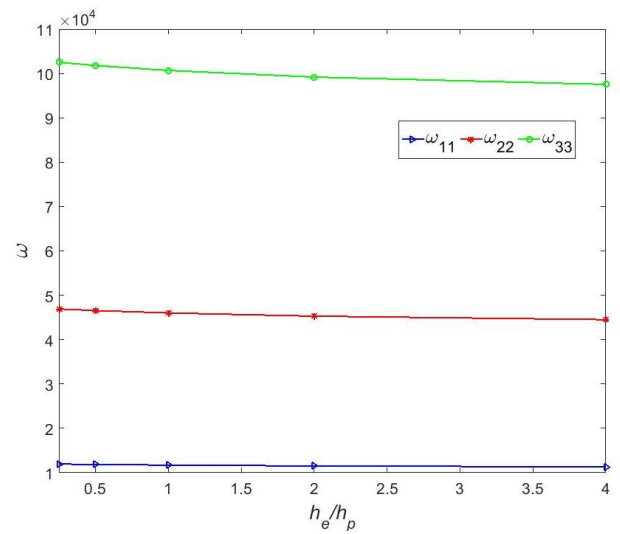

Fig. 3 Variation of first, second and third natural frequencies of sandwich porous plate in terms of h_e/h_p ratio

Table 3 Variation of natural frequencies in terms of various values of he/hp for different porosities

ratio	0.25	0.5	1	2	**4**
Uniform	15290.323	15002.423	14578.553	14069.140	**13521.955**
Nonuniform	15292.383	15012.884	14631.042	14201.908	**13811.385**
Nonuniform2	15290.971	15005.076	14597.439	14096.757	**13576.943**

Table 4 Variation of fundamental natural frequencies of sandwich porous plate in terms of various a/h for different porosity distributions

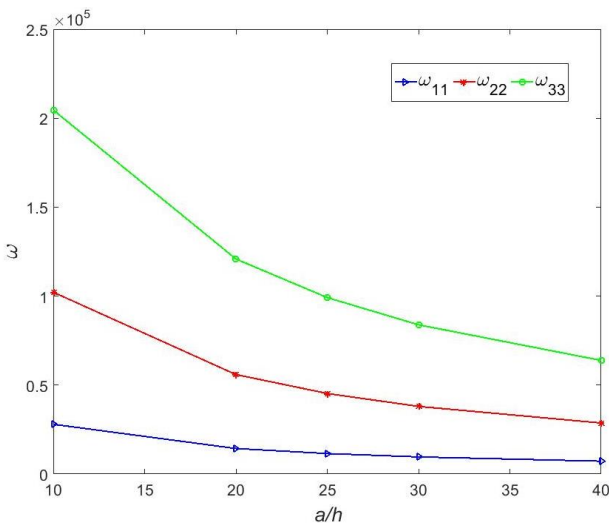| a/h	10	20	25	30	**40**
Uniform	33941.440	17516.584	14069.140	11749.857	**8831.616**
Nonuniform1	34238.513	17680.493	14201.908	11861.255	**8915.735**
Nonuniform2	34008.111	17550.969	14096.757	11772.922	**8848.952**

Fig. 4 Variation of first, second and third natural frequencies of sandwich porous plate in terms of various values of side length to thickness ratio a/h

One can conclude that with increase of side length to thickness ratio a/h, the fundamental natural frequencies are decreased significantly. One can conclude that with increase of a/h, the stiffness of plate is decreased that leads to decrease of natural frequencies.

Shown in Figure 4 is variation of first, second and third natural frequencies of sandwich porous plate in terms of various values of side length to thickness ratio a/h. it is observed that with increase of a/h ratio, the stiffness of sandwich plate is decreased and consequently the natural frequencies are decreased significantly.

Table 5 lists variation of fundamental natural frequencies of sandwich porous plate in terms of various coefficients of porosity e_0 for various porosity distributions. The numerical results indicate that with increase of coefficients of porosity e_0, the natural frequencies are increased significantly. One can conclude that with increase of coefficients of porosity e_0, the stiffness of porous material is increased.

Table 5 Variation of fundamental natural frequencies of sandwich porous plate in terms of various coefficients of porosity e_0 for various porosity distributions

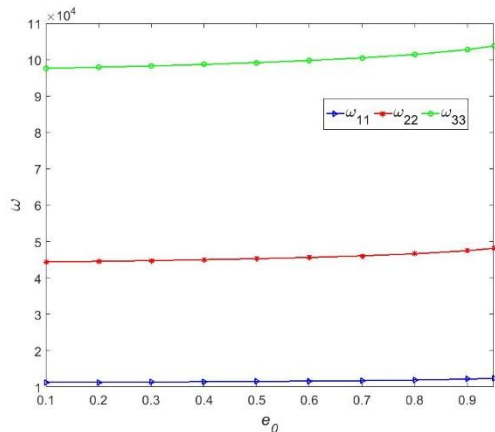| Ratio	0	0.2	0.4	0.6	0.8	0.95
Uniform	13705	13931	14229	14651	15345	16494
Nonuniform1	13705	14014	14420	14997	15959	17611
Nonuniform2	13507	13948	14270	14730	15503	16833

Fig. 5 Variation of first, second and third natural frequencies of sandwich porous plate in terms of various coefficients of porosity e_0

Fig. 6 Effect of the axial wave number and electric potentials on the frequency of sandwich micro plate

Figure 5 shows variation of first, second and third natural frequencies of sandwich porous plate in terms of various coefficients of porosity e_0. It is observed that with increase of coefficients of porosity e_0, the stiffness of material is increased and then the natural frequencies are increased.

In Figure 6 influence of the electric potentials and axial wave number on the frequency parameter ($\omega/\omega_{\Psi=0}$) of sandwich micro plate is presented. Also, $\omega_{\Psi=0}$ is the natural frequency of the of sandwich porous plate when $\Psi = 0$. That with increase of the n the frequency parameter $\omega/\omega_{\Psi=0}$ increased. Also, with increase of the electric potentials the fundamental frequency parameter decreased.

5. Conclusion

Free vibration analysis of a sandwich porous plate was studied in this paper using the hyperbolic shear deformation theory. The total transverse displacement of sandwich pate was assumed as summation of two portions; one related to bending deformation and another to shear deformation. Hamilton's principle and piezo elasticity relations were used to derive governing equations of motion. The numerical results were presented based on analytical solution of the governing equations of motion. The numerical results indicate that some significant parameters of the problem play an important role on the change of outputs. Some important conclusions of this study is presented as follows:

The influence of coefficients of porosity e_0 was studied on the free vibration characteristics of sandwich porous
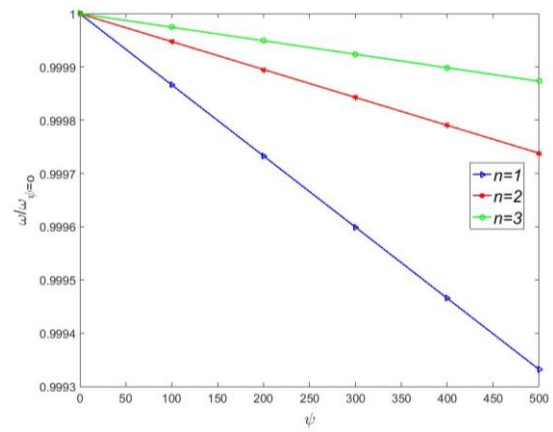
plate. One can conclude that with increase of coefficients of porosity e_0, the stiffness of material is increased and then the natural frequencies are increased. In addition, the influence of type of porosity distribution was studied on the responses. It is observed that the second distribution (Nonuniform1) yields highest natural frequency and lowest one is obtained for first distribution (Uniform).

The influence of dimensionless geometric parameters was studied on the responses of system. One can conclude that with increase of side length to thickness ratio a/h and core thickness to piezoelectric thickness ratio h_e / h_p, the stiffness of structure is decreased that leads to decrease of natural frequencies. In addition, the influence of side lengths ratio a/b was studied on the responses. It is concluded that minimum natural frequency is obtained for square plate (a/b=1). For other ratios of a/b, the natural frequencies are increased significantly.

References

Abbas, I., Hamdy, A. and Youssef, M. (2015), "Two-dimensional fractional order generalized thermoelastic porous material", *Lat. Am. J. Solid. Struct.*, **12**(7), 1415-1431. http://doi.org/10.1590/1679-78251584.

Ait Atmane, H., Tounsi, A. and Bernard, F. (2017), "Effect of thickness stretching and porosity on mechanical response of a functionally graded beams resting on elastic foundations", *J. Mech. Mater. Des.*, **13**(1), 71-84. https://doi.org/10.1007/s10999-015-9318-x.

Arefi, M. and Rahimi, G.H. (2012), "Three-dimensional multi-field equations of a functionally graded piezoelectric thick shell with variable thickness, curvature and arbitrary nonhomogeneity", *Acta. Mech.* **223**(1), 63-79. https://doi.org/10.1007/s00707-011-0536-5.

Arefi, M. (2016), "Analysis of wave in a functionally graded magneto-electro-elastic nano-rod using nonlocal elasticity model subjected to electric and magnetic potentials", *Acta. Mech.*, **227**(9), 2529-2542. https://doi.org/10.1007/s00707-016-1584-7.

Arefi, M. and Zenkour, A.M. (2017a), "Effect of thermos magneto-electro mechanical fields on the bending behaviors of a three-layered nanoplate based on sinusoidal shear deformation plate theory", *J. Sandw. Struct. Mater.,* **56**, 1-31. https://doi.org/10.1177/1099636217697497.

Arefi, M. and Zenkour, A.M. (2017b), "Influence of micro-length-scale parameters and inhomogeneities on the bending, free

vibration and wave propagation analyses of a FG Timoshenko's sandwich piezoelectric microbeam", *J. Sandw. Struct. Mater.,* https://doi.org/10.1177/1099636217714181.

Arefi, M. and Zenkour, A.M. (2017c), "Size-dependent free vibration and dynamic analyses of piezo-electro-magnetic sandwich nanoplates resting on viscoelastic foundation", *Phys. B: Cond. Mat.,* **521**, 188-197. https://doi.org/10.1016/j.physb.2017.06.066.

Arefi, M. and Zenkour, A.M. (2018), "Employing the coupled stress components and surface elasticity for nonlocal solution of wave propagation of a functionally graded piezoelectric love nanorod model", *J. Intel. Mater. Syst. Struct.,* **28**(17), 2403-2413. https://doi.org/10.1177/1045389X17689930.

Arefi, M., Zamani, M.H. and Kiani, M. (2018), "Size-dependent free vibration analysis of three-layered exponentially graded nanoplate with piezomagnetic face-sheets resting on Pasternak's foundation", *J. Intel. Mater. Syst. Struct.,* **29**(5), 774-786.

Arefi, M. (2018a), "Analysis of a doubly curved piezoelectric nano shell: nonlocal electro-elastic bending solution", *Eur. J. Mech-A/Solids,* **70**, 226-237. https://doi.org/10.1016/j.euromechsol.2018.02.012.

Arefi, M. (2018b), "Buckling analysis of the functionally graded sandwich rectangular plates integrated with piezoelectric layers under bi-axial loads", *J. Sandw. Struct. Mater.,* **19**(6), 712-735. https://doi.org/10.1177/1099636216642393.

Barati, M.R. and Zenkour, A.M. (2017), "Investigating post-buckling of geometrically imperfect metal foam Nano beams with symmetric and asymmetric porosity distributions", *Compos. Struct.,* **182**, 91-98. https://doi.org/10.1016/j.compstruct.2017.09.008.

Benachour, A., Tahar, H.D., Atmane, H.A., Tounsi, A. and Ahmed, M.S. (2011), "A four variable refined plate theory for free vibrations of functionally graded plates with arbitrary gradient", *Compos. Part B. Eng.,* **42**(6), 1386-1394. https://doi.org/10.1016/j.compositesb.2011.05.032.

Benahmed, A., Houari, M.S.A., Benyoucef, S., Elakhdar, K. and Tounsi, A. (2017), "A novel quasi-3D hyperbolic shear deformation theory for functionally graded thick rectangular plates on elastic foundation", *Geomech. Eng.,* **12**(1), 9-34. https://doi.org/10.12989/gae.2017.12.1.009.

Chen, D., Yang, J. and Kitipornchai, S. (2019), "Buckling and bending analyses of a novel functionally graded porous plate using Chebyshev-Ritz method", *Civil Mech. Eng.,* **19**(1), 157-170. https://doi.org/10.1016/j.acme.2018.09.004.

Chen, L.W., Lin, C.Y. and Wang, C.C. (2002), "Dynamic stability analysis and control of a composite beam with piezoelectric layers", *Compos. Struct.,* **56**(1), 97-109. https://doi.org/10.1016/S0263-8223(01)00183-0.

Demirhan, P.A. and Taskin, V. (2018), "Bending and free vibration of levy-type porous functionally graded plate using state space approach", *Compos. Part B,* **160**, https://doi.org/10.1016/j.compositesb.2018.12.020.

Ebrahimi, F. and Habibi, S. (2016), "Deflection and vibration analysis of higher-order shear deformable compositionally graded porous plate", *Steel. Compos. Struct.,* **20**(1), 150-162. http://dx.doi.org/10.12989/scs.2016.20.1.205.

El Meiche, N., Tounsi, A., Ziane, N., Mechab, I. and Bedia, E.A.A. (2011), "A new hyperbolic shear deformation theory for buckling and vibration of functionally graded sandwich plate", *Int. J. Mech. Sci.,* **53**(4), 237-247. https://doi.org/10.1016/j.ijmecsci.2011.01.004.

Fakhari, V., Ohadi, A. and Yousefian, P. (2011), "Nonlinear free and forced vibration behavior of functionally graded plate with piezoelectric layer in thermal environment", *Compos. Struct.,* **93**(9), 2310-2321. https://doi.org/10.1016/j.compstruct.2011.03.019.

Galeban, M.R. Mojahedin, A. Taghavi Y. and Jabbari, M. (2016), "Free vibration of functionally graded thin beams made of

saturated porous materials", *Steel. Compos. Struct.,* **21**(5), 25-36. https://doi.org/10.12989/scs.2016.21.5.999.

Hebali, H., Tounsi, A., Houari, M.S.A., Bessaim, A. and Bedia, E.A.A. (2014), "New quasi-3D hyperbolic shear deformation theory for the static and free vibration analysis of functionally graded plates", *J. Eng. Mech.* **140**(2), 374-383. https://doi.org/10.1061/(ASCE)EM.1943-7889.0000665.

Khorshidi, K., Asgari, T. and Fallah, A. (2015), "Free vibrations analysis of functionally graded rectangular nano-plates based on nonlocal exponential shear deformation theory", *Mech. Adv. Compos. Struct.,* **2**(2), 79-93. http://dx.doi.org/10.22075/macs.2015.395.

Kim, J., Zur, K.K. and Reddy, J. N (2019), "Bending, free vibration, and buckling of modified couples stress-based functionally graded porous micro-plates", *Comp. Struct.,* **209**, 879-888. https://doi.org/10.1016/j.compstruct.2018.11.023.

Li, K., Wu, D., Chen, X., Cheng, J., Liu, Z., Gao, W. and Liu, M. (2018), "Isogeometric Analysis of functionally graded porous plates reinforced by graphene platelets", *Comp. Struct.,* **204**, 114-130. https://doi.org/10.1016/j.compstruct.2018.07.059.

Li, L., Hu, Y. and Ling, L. (2015), "Flexural wave propagation in small-scaled functionally graded beams via a nonlocal strain gradient theory", *Compos. Struct.,* **1**(133), 1079-1092. https://doi.org/10.1016/j.compstruct.2015.08.014.

Li, L., Hu, Y. and Ling, L. (2016), "Wave propagation in viscoelastic single-walled carbon nanotubes with surface effect under magnetic field based on nonlocal strain gradient theory", *Phys. E.,* **75**, 118-124. https://doi.org/10.1016/j.physe.2015.09.028.

Lim, C.W., Zhang, G. and Reddy, J.N. (2015), "A higher-order nonlocal elasticity and strain gradient theory and its applications in wave propagation", *J. Mech. Phys. Solids,* **78**, 298-313. https://doi.org/10.1016/j.jmps.2015.02.001.

Mechab, I., Mechab, B., Benaissa, S., Serier, B. and Bouiadjra, BB. (2016), "Free vibration analysis of FGM nanoplate with porosities resting on Winkler Pasternak elastic foundations based on two-variable refined plate theories", *J. Braz. Soc. Mech. Sci. Eng.,* **38**(8), 2193-2211. https://doi.org/10.1007/s40430-015-0482-6.

Mehralian, F., Beni, Y.T. and Zeverdejani, M.K. (2017), "Nonlocal strain gradient theory calibration using molecular dynamics simulation based on small scale vibration of nanotubes", *Phys. B. Condens. Matter,* **514**, 61-69. https://doi.org/10.1016/j.physb.2017.03.030.

Reddy, J.N. (2004), *Mechanics of Laminated Composite Plates and Shells Theory and Analysis,* 2*nd Ed.*, CRC Press, Florida, USA.

Mirjavadi, S.S. Afshari, B.M. Shafiei, N. Hamouda, A.M.S. and Kazemi, M. (2017), "Thermal vibration of two-dimensional functionally graded (2D-FG) porous Timoshenko nanobeams", *Steel. Compos. Struct.* **25**(4), 55-67. https://doi.org/10.12989/scs.2017.25.4.415.

Rezaei, A.S. and Saidi, A.R. (2016), "Application of Carrera Unified Formulation to study the effect of porosity on natural frequencies of thick porous–cellular plates", **91**, *Compos. Part B Eng.,* **91**, 361-370. https://doi.org/10.1016/j.compositesb.2015.12.050.

Wu, X.H., Chen, C.Q., Shen, Y.P. and Tian, X.G. (2002), "A high order theory for functionally graded piezoelectric shells", *J. Solid. Struct.,* **39**(20), 5325-5344. https://doi.org/10.1016/S0020-7683(02)00418-3.

Zhao, J., Wang, Q., Deng, X., Choe, K., Zhong, R. and Shuai, C. (2018), "Free vibrations of functionally graded porous rectangular plate with uniform elastic boundary conditions", *Compos. Part B,* **168**, 106-120. https://doi.org/10.1016/j.compositesb.2018.12.044.

CC

Appendix 1

In this appendix the variation of strain energy (U) is defined as follows:

$$\delta U = \left(-\frac{\partial N_x}{\partial x}\delta u_0 - \frac{\partial^2 M_x^b}{\partial^2 x}\delta w_b - \frac{\partial^2 M_x^s}{\partial^2 x}\delta w_s \right)$$

$$+\left(-\frac{\partial N_y}{\partial y}\delta v_0 - \frac{\partial^2 M_y^b}{\partial^2 y}\delta w_b - \frac{\partial^2 M_y^s}{\partial^2 y}\delta w_s \right)$$

$$+\left(-\frac{\partial N_{xy}}{\partial y}\delta u_0 - \frac{\partial N_{xy}}{\partial x}\delta v_0 - 2\frac{\partial^2 M_{xy}^b}{\partial x\,\partial y}\delta w_b - 2\frac{\partial^2 M_{xy}^s}{\partial x\,\partial y}\delta w_s \right)$$

$$+\left(-\frac{\partial S_{xz}}{\partial x}\delta w_s - \frac{\partial S_{xz}}{\partial x}\delta\varphi \right)+$$

$$\left(-\frac{\partial S_{yz}}{\partial y}\delta w_s - \frac{\partial S_{yz}}{\partial y}\delta\varphi \right)+\frac{\partial P_x}{\partial x}\delta\psi + \frac{\partial P_y}{\partial y}\delta\psi + R_z\delta\psi$$

Appendix 2

In this appendix the variation of kinetic energy (T) is defined as follows:

$$\delta T = -I_1\ddot{u}\,\delta u_0 - I_2\ddot{u}_{0,x}\,\delta w_b - I_4\ddot{u}_{0,x}\,\delta w_s + I_2\ddot{w}_{b,x}\,\delta u_0$$

$$+I_3\ddot{w}_{b,xx}\,\delta w_b + I_5\ddot{w}_{b,xx}\,\delta w_s + I_4\ddot{w}_{s,x}\,\delta u_0$$

$$+I_5\ddot{w}_{s,xx}\,\delta w_b + I_6\ddot{w}_{s,xx}\,\delta w_s - I_2\ddot{v}_0\,\delta v_0 - I_2\ddot{v}_{0,y}\,\delta w_b$$

$$-I_4\ddot{v}_{0,y}\,\delta w_s + I_2\ddot{w}_{b,y}\,\delta v_0 + I_3\ddot{w}_{b,yy}\,\delta w_b +$$

$$I_5\ddot{w}_{b,yy}\,\delta w_s + I_4\ddot{w}_{s,y}\,\delta v_0 + I_5\ddot{w}_{s,yy}\,\delta w_b + I_6\ddot{w}_{s,yy}\,\delta w_s$$

$$-I_1\ddot{w}_b\,\delta w_b - I_1\ddot{w}_b\,\delta w_s - I_7\ddot{w}_b\,\delta\varphi - I_1\ddot{w}_s\,\delta w_b$$

$$-I_1\ddot{w}_s\,\delta w_s - I_7\ddot{w}_s\,\delta\varphi - I_7\ddot{\varphi}\,\delta w_b - I_7\ddot{\varphi}\,\delta w_s - I_8\ddot{\varphi}\,\delta\varphi$$

Appendix 3

In this appendix the component of K, M is defines as follows.

$$K_{11} = -A_{11}\lambda^2 - A_{66}\mu^2, K_{12} = K_{12} = -A_{12}\lambda\mu - A_{66}\lambda\mu$$

$$K_{13} = K_{31} = B_{11}\lambda^3 + B_{12}\lambda\mu^2 + 2B_{66}\lambda\mu^2$$

$$K_{14} = K_{41} = E_{11}\lambda^3 + E_{12}\lambda\mu^2 + 2B_{66}\lambda\mu^2$$

$$K_{15} = K_{51} = 0, K_{16} = K_{61} = K_{13}^1\lambda, K_{22} = -A_{66}\lambda^2 - A_{22}\mu^2$$

$$K_{23} = K_{32} = 2B_{66}\lambda^2\mu + B_{12}\lambda^2\mu + B_{22}\mu^3$$

$$K_{24} = K_{42} = 2E_{66}\lambda^2\mu + E_{12}\lambda^2\mu + E_{22}\mu^3$$

$$K_{25} = K_{52} = 0, K_{26} = K_{62} = -K_{23}^1\mu$$

$$K_{33} = -D_{11}\lambda^4 - D_{22}\mu^4 - 2D_{12}\lambda^2\mu^2 - 4D_{66}\lambda^2\mu^2$$

$$K_{34} = K_{43} = -F_{11}\lambda^4 - F_{22}\mu^4 - 2F_{12}\lambda^2\mu^2 - 4F_{66}\lambda^2\mu^2$$

$$K_{35} = K_{53} = 0, K_{36} = K_{63} = K_{23}^2\mu^2 + K_{13}^2\lambda^2$$

$$K_{44} = -2G_{12}\lambda^2\mu^2 - 2G_{66}\lambda^2\mu^2 - G_{22}\mu^4 - H_{44}\lambda^2 - H_{55}\mu^2$$

$$K_{45} = K_{54} = -H_{44}\lambda^2 - H_{55}\mu^2, K_{46} = K_{64} = -K_{13}^4\lambda^2 - K_{23}^4\mu^2 + L_{51}^3\lambda^2 + L_{62}^3\mu^2$$

$$K_{55} = -H_{44}\lambda^2 - H_{55}\mu^2, K_{56} = K_{65} = L_{51}^3\lambda^2 + L_{62}^3\mu^2$$

$$K_{66} = -L_{11}^5\lambda^2 - L_{22}^5\mu^2 - K_{33}^5$$

$$M_{11} = -w^2 I_1, \quad M_{12} = M_{21} = 0, \quad M_{13} = M_{31} = w^2\lambda I_2, \quad M_{14} = M_{41} = w^2\lambda I_4$$

$$M_{15} = M_{51} = M_{16} = M_{61} = 0, \quad M_{22} = -w^2 I_1, \quad M_{23} = M_{32} = w^2\mu I_2$$

$$M_{24} = M_{42} = w^2\mu I_4, M_{25} = M_{52} = 0, \quad M_{26} = M_{62} = 0$$

$$M_{33} = -w^2 I_1 - w^2\lambda I_3 - w^2\mu I_4, \quad M_{34} = M_{43} = -w^2\lambda I_5 - w^2\mu I_5 - w^2 I_1$$

$$M_{35} = M_{53} = -w^2 I_7, M_{36} = M_{63} = 0, \quad M_{44} = -w^2 I_1 - w^2\lambda^2 I_6 - w^2\mu^2 I_6$$

$$M_{45} = M_{54} = -w^2 I_7, M_{46} = M_{64} = 0, \quad M_{55} = -w^2 I_8, M_{56} = M_{65} = M_{66} = 0$$